SUPPLEMENTAL MATERIAL

Mortensen et al., http://www.jem.org/cgi/content/full/jem.20101145/DC1

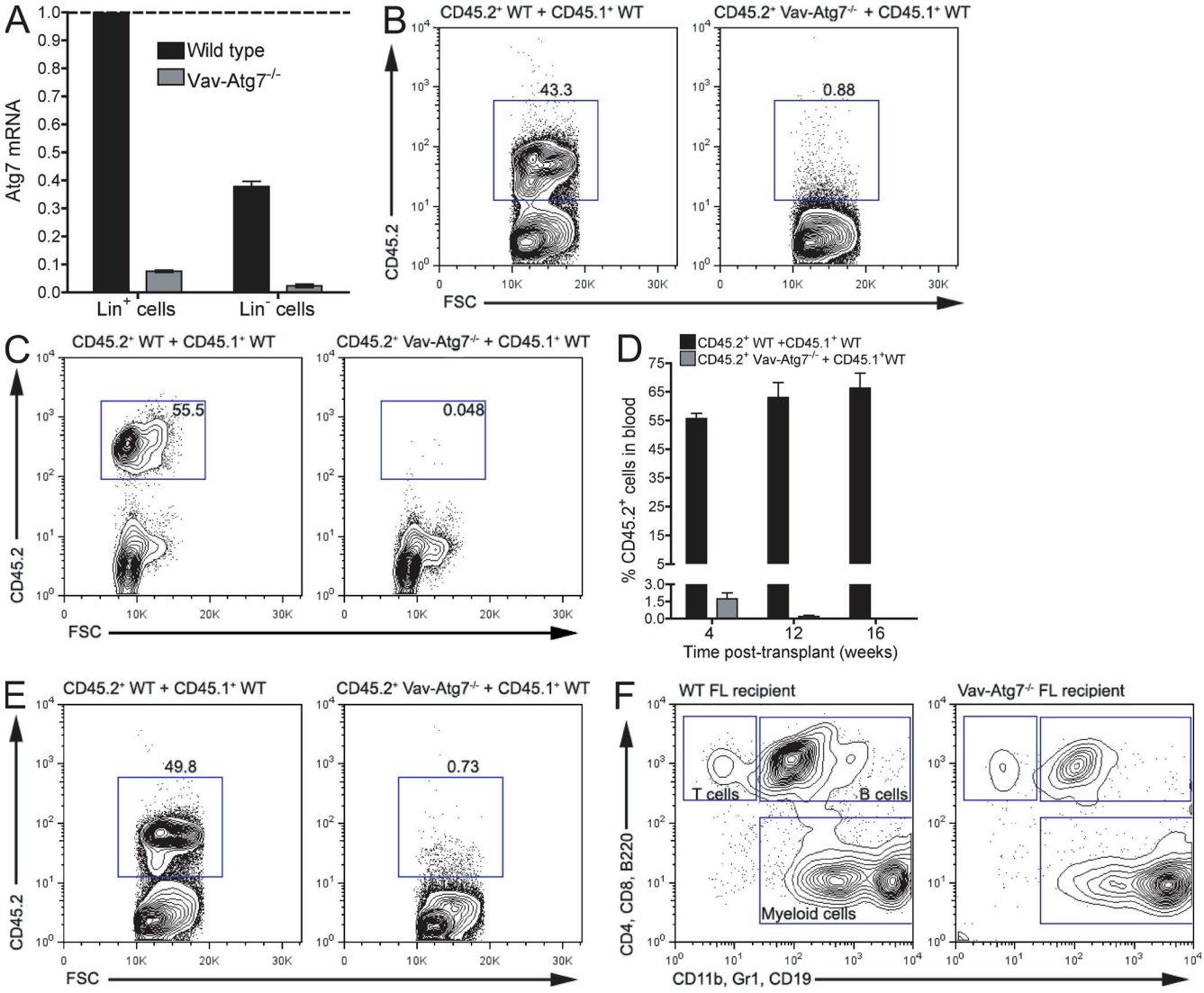

Figure S1. In vivo reconstitution assays. (A) Relative Atg7 messenger RNA (mRNA) expression was measured by real-time Q-PCR in Lin^+ and Lin^- BM cells in WT and Vav-$Atg7^{-/-}$ mice. Error bars indicate SEM. (B) Representative dot plots of $CD45.2^+$ cells in the BM of recipients shown in Fig. 1 (D and E). The mice were analyzed 17 wk after transplantation. BM cells from 6-wk-old WT (left) and Vav-$Atg7^{-/-}$ BM (right) mice were mixed with $CD45.1^+$ support BM cells in a 1:1 ratio and transplanted into lethally irradiated recipients ($n = 7$ per group). (C) Representative dot plots showing the percentage of $CD45.2^+$ cells in peripheral blood of recipient mice. The analysis was performed 16 wk after transplantation. The $CD45.2^+$ population frequency is shown within the gate. (D) Mean percentage (±SEM) of $CD45.2^+$ cells (gated as shown in C) in peripheral blood of the recipient mice. The analysis was performed at 4, 12, and 16 wk after transplantation. (E) Donor-derived $CD45.2^+$ cells in the BM of lethally irradiated BM transplant recipients 17 wk after transplantation. Representative dot plots are shown. (F) Representative dot plots showing the reconstitution of T (CD4 and CD8), B (B220 and CD19), and myeloid cells (CD11b and Gr1) by donor-derived $CD45.2^+$ cells in the blood of FL chimeras from Fig. 1 (I and J) 4 wk after transplant.

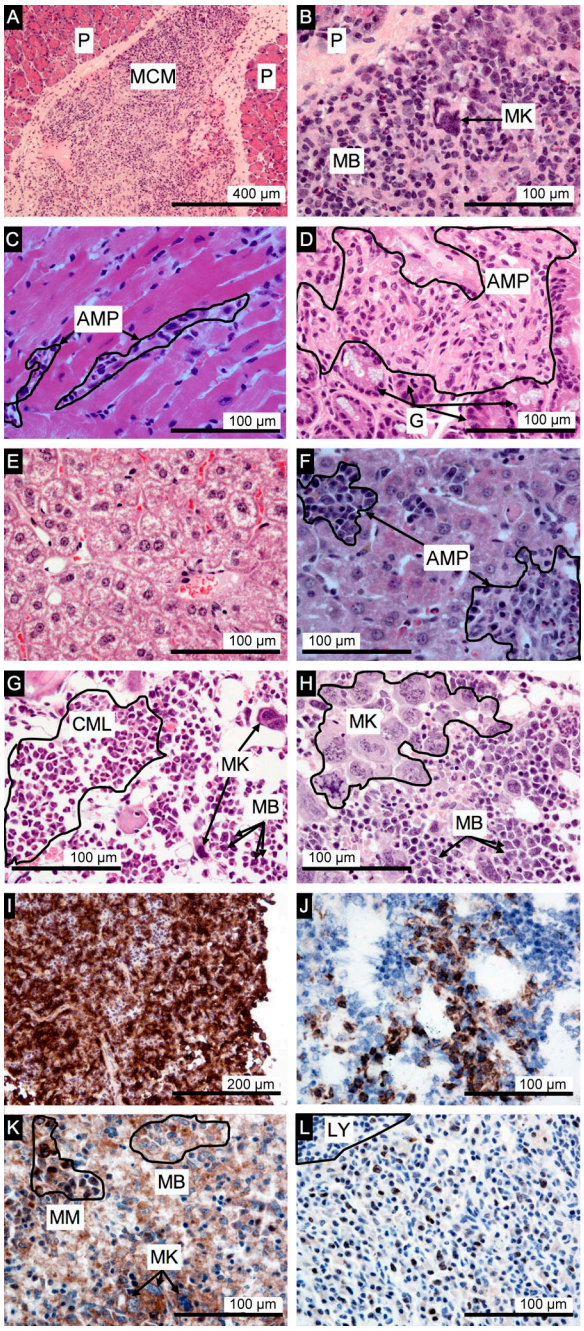

Figure S2. Vav-Atg7$^{-/-}$ mice present myeloid infiltrates in a wide range of organs. (A) H&E-stained section of the myeloid cell mass (MCM) in the pancreas (P). (B) Higher power magnification of the myeloid cell mass from A. The mass is composed of atypical hematopoietic cells with irregular nuclei, many of which have a high nuclear/cytoplasmic ratio and prominent nucleolus, which is typical of myeloid blast cells (MB) and atypical megakaryocytes (MK). (C) Vav-Atg7$^{-/-}$ heart section. Atypical myeloid proliferation (AMP) found between muscle fibers of the heart. (D) Vav-Atg7$^{-/-}$ small intestine section. Atypical myeloid proliferation destroying small intestinal glands (G)/villi shows bean-shaped nuclei and abundant cytoplasm, which is indicative of myelomonocytic differentiation. (E) WT H&E-stained liver. (F) Atypical myeloid proliferation in Vav-Atg7$^{-/-}$ liver. (G) BM from Vav-Atg7$^{-/-}$ (5) mouse described in Table S2 with abundant chronic myeloid leukemia-like maturing myeloid cells (CML), atypical megakaryocytes, and smaller numbers of myeloid blast cells. (H) BM from Vav-Atg7$^{-/-}$ (1) mouse described in Table S2 with abundant essential thrombocythemia-like, hyperlobated, atypical megakaryocytes, together with large numbers of myeloid blast cells. All sections shown in (A–H) are H&E-stained, formalin-fixed, paraffin-embedded material from 9- or 10-wk-old Vav-Atg7$^{-/-}$ mice, unless stated otherwise. (I) CD68 immunostaining on the pancreatic cell mass from A and B. CD68 immunostains the majority of the cells. (J) CD11b immunostaining on frozen sections of the cell mass shown in A and B. (K) Myeloperoxidase immunostaining of a Vav-Atg7$^{-/-}$ spleen paraffin section. Myeloperoxidase stains maturing myeloid cells (MM) of the myeloid infiltrates strongly, while showing weak staining of atypical megakaryocytes and patchy weak staining of some myeloid blast cells. (L) Immunostaining of a Vav-Atg7$^{-/-}$ lymph node. Ki67 (brown) immunostains 30–80% (here ∼40%) of the infiltrating myeloid cells. Residual lymphocytes (LY) are present in this largely infiltrated lymph node.

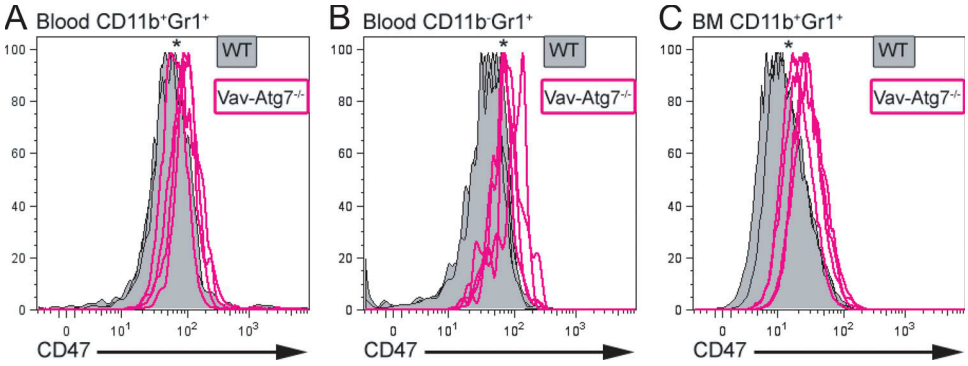

Figure S3. Myeloid cells from Vav–Atg7$^{-/-}$ mice express higher levels of the myeloid leukemia marker CD47. (A and B) CD47 expression on blood CD11b^{+}Gr1^{+} (A) and CD11b^{-}Gr1^{+} (B) cells (gated as shown in Fig. 6 A) from 7-wk-old WT (n = 5) and Vav-Atg7$^{-/-}$ (n = 4) mice. (C) CD47 expression on BM CD11b^{+}Gr1^{+} cells (gated as shown in Fig. 6 B) from 9-wk-old WT (n = 5) and Vav-Atg7$^{-/-}$ (n = 4) mice. *, P < 0.05 from Mann-Whitney test on the fluorescence geometric mean of CD47.

Table S1. Organs presenting myeloid infiltrates in 9–10-wk-old Vav-Atg7$^{-/-}$ mice at autopsy

Organs	Number of Vav–Atg7$^{-/-}$ mice presenting with myeloid infiltrates
Thymus	2
Spleen	5
Lymph nodes	5
Liver	5
Intestines	5
Lungs	4
Skin	4
Heart	4
Pancreas	4
Kidney	2

All organs were examined for n = 6 Vav-Atg7$^{-/-}$ mice, except for the lungs, which were examined for n = 5 Vav-Atg7$^{-/-}$ mice.

Table S2. Histological features of sternal BM in the six Vav-Atg7$^{-/-}$ mice analyzed for myeloid infiltrates

Mouse	Histological features of BM	Marrow cellularity	Morphological % of blast cells	Myeloid cells	Erythroid cells	Megaka ryocytes	Comments
		%	%	%	%	%	
Vav-Atg7$^{-/-}$ (1)	Acute myeloid leukemia-like cells arising in an essential thrombocytopenia-like chronic MPD.	95	40	>70	10–20	10–20	No obvious fibrosis. Very patchy distribution of megakaryocytes. Very significant myeloid and megakaryocytic dysplasia with micromegakaryocytes.
Vav-Atg7$^{-/-}$ (2)	Myelodysplastic features, but no acute myeloid leukemia-like features.	95	10–15	90	<10	5–10	No obvious fibrosis. Very significant myeloid and megakaryocytic dysplasia with micromegakaryocytes. Occasional erythroid cells remain.
Vav-Atg7$^{-/-}$ (3)	Acute myeloid leukemia-like features arising in a chronic myeloid leukemia-like chronic MPD.	100	20	>95	<5	1–2	No obvious fibrosis. Large numbers of slightly immature neutrophils.
Vav-Atg7$^{-/-}$ (4)	Acute myeloid leukemia-like features arising on a severely myelodysplastic background.	100	30	>90	<5	5–10	No obvious fibrosis. Diffuse distribution of megakaryocytes. Very significant myeloid and megakaryocytic dysplasia with micromegakaryocytes.
Vav-Atg7$^{-/-}$ (5)	Acute myeloid leukemia-like arising in a chronic myeloid leukemia-like chronic MPD.	100	20-30	>95	<5	2–3	As for Vav-Atg7$^{-/-}$ (3).
Vav-Atg7$^{-/-}$ (6)	Acute myeloid leukemia-like features arising in an essential thrombocytopenia-like chronic MPD.	100	40–50	80–85	<5	10–15	As for Vav-Atg7$^{-/-}$ (1)
WT (n = 3)	Normal features.	95–100	<5	80	15–20	2–5	No fibrosis.

Table S3. Transplantability of the myeloproliferation from Vav-Atg7$^{-/-}$ in the different transplantation settings

Experimental setting	Recipient strain	Cell type	Cells injected	Irrad iation	Number of recipient mice	Myeloproliferation in peripheral hematopoietic organs of recipients of Vav-Atg7$^{-/-}$ cells	Myelodysplasia in BM	Symptoms and time of culling of recipients of Vav-Atg7$^{-/-}$ cells	Hematopoietic reconstitution by Vav-Atg7$^{-/-}$ cells
1:1 competitive BM repopulation assay	B6SJL CD45.1	BM	1 × 10^6 test + 1 × 10^6 CD45.1$^+$	Lethal	6 WT; 6 Vav-Atg7$^{-/-}$	No	N/A	N/A	No
BM transplant into immunocompromised mice	Rag-1$^{-/-}$	BM	2 × 10^6	Sublethal	2 WT; 4 Vav-Atg7$^{-/-}$	Yes in 4/4	No	No in 12 wk	N/A
Noncompetitive BM repopulation assay	B6SJL CD45.1	BM	2 × 10^6	Lethal	2 WT; 3 Vav-Atg7$^{-/-}$	Yes in 3/3	No[a]	Yes in 4 wk	Short term only
Noncompetitive FL repopulation assay	B6SJL CD45.1	FL	2 × 10^6	Lethal	5 WT; 6 Vav-Atg7$^{-/-}$	Yes in 4/6	Yes in 2/4 recipients with myeloproliferation	Yes in 7 wk (only the 4 recipients with myeloproliferation)	Yes, but not as efficient as from WT FL cells
LSK cell repopulation assay	B6SJL CD45.1	BM LSK cells	1 × 10^4	Lethal	3 WT; 5 Vav-Atg7$^{-/-}$	Yes in 2/2 (only 2/5 were analyzed)	No[a]	Yes in 15 d	No

N/A, not applicable. For Myeloproliferation in peripheral hematopoietic organs of recipients of Vav-Atg7$^{-/-}$ cells, the organs examined were the thymus, lymph nodes, spleen, and liver.

[a]The BM of these mice displayed low cellularity, indicating poor or no BM repopulation.